Available online at www.sciencedirect.com
ScienceDirect
Ceramics International 35 (2009) 1617–1623
CERAMICS INTERNATIONAL
www.elsevier.com/locate/ceramint

Composites from WC powders sputter-deposited with iron rich binders

C.M. Fernandes [a], A.M.R. Senos [a,*], M.T. Vieira [b], J.V. Fernandes [b]

[a] Department of Ceramics and Glass Engineering, CICECO, University of Aveiro, 3810-193 Aveiro, Portugal
[b] CEMUC – Mechanical Engineering Department, University of Coimbra, Rua Luís Reis Santos, Pinhal de Marrocos, 3030-788 Coimbra, Portugal

Received 9 July 2008; received in revised form 22 July 2008; accepted 8 September 2008
Available online 8 October 2008

Abstract

Composite powders of tungsten carbide (WC) and iron rich binder were prepared by an innovative approach, which consists in sputtering of a metallic binder on the tungsten carbide particles. The phase composition, microstructure and mechanical behaviour of WC coated powder composites with binder contents from 6 to 9 wt.% were characterized. η-Phase is early formed during sintering and its effect on the mechanical behaviour was investigated and related to the microstructure and atomic structure. The results show that the presence of η-phase has not a hazardous role in toughness as is previewed in conventional cemented carbide. Despite the presence of η-phase, a good compromise between toughness and hardness was attained in composites prepared from iron rich binders sputtered on WC powders.

Keywords: C. Mechanical properties; C. Hardness; D. Carbides; Sputter-coated powders

1. Introduction

Hard metals are commonly manufactured with tungsten carbide (WC) and cobalt as metallic binder. Due to the unique mechanical properties of this composite it has not been easy to find a good substitute, in spite of the several studies with other transition metals in the neighbourhood of cobalt, as iron or nickel [1–6].

Fe–Cr–Ni–C alloys, as stainless steel, have been studied for cobalt substitution [7–11]. The binder was added to WC by an innovative way, which consists in sputtering austenitic stainless steel on the tungsten carbide particles. The coated powders have a good pressing behaviour, which allows the direct pressing without the need of the usual paraffin wax [7–11]. Moreover, the nanocristallinity of these coatings, together with the good distribution of the binder, increases the reactivity of the powders and consequently decreases the sintering temperature needed to attain dense specimens [9,12]. Nevertheless, binders enriched in iron induce the formation of a brittle η-carbide M_6C, which is generally considered an undesirable phase in tungsten carbide, as it is expected to markedly reduce the toughness, comparatively to cemented carbides free of this phase [13–15]. However, η-carbide was already mentioned in 1950s as a possible raw material to improve hardness in cemented carbide [16], but neither this potential advantage of η-phase was further explored, nor its negative effects in the mechanical properties have been determined and related to the phase composition and microstructure of the composites.

In this work, the feasibility of Fe/Ni/Cr-based alloys as binders in cemented carbides and sputtering as an alternative to the conventional powder mixture will be investigated. For such purpose, the effect of the binder composition and, consequently, of the η-phase content in the final mechanical properties will be evaluated in composites obtained from sputter coated powders and from a conventional mixture, used as standard.

2. Experimental

The starting powder is a fully carburized WC (H.C. Starck, HCST-Germany) with an average particle diameter of 9.06 ± 0.47 μm. Composite powders were prepared by coating the WC particles with the metallic binder, using a modified d.c. magnetron sputtering deposition chamber with deposition parameters reported elsewhere [7]. Two different targets were used; a stainless steel (SS) AISI 304 and a SS composed with a pathwork of Ni discs (in order to increase the sputtered Ni

* Corresponding author. Tel.: +351 234 370 354; fax: +351 234 370 204.
E-mail address: anamor@ua.pt (A.M.R. Senos).

0272-8842/$34.00
doi:10.1016/j.ceramint.2008.09.009

content of SS). A conventional mixture was also prepared with 1.5 wt.% of paraffin wax, the same WC powder and a SS powder (Goodfellow FE226010, maximum particle size of 45 μm) by wet milling, using isopropyl alcohol in a stainless steel mill with WC–Co balls, during 6 h. After mixing, the mixture was dried, deagglomerated and sieved.

Two coated powders have been prepared. The first one, coated with SS, was designated by C-WC1. After unidirectional pressing at 190 MPa, the compacts were vacuum sintered at a maximum temperature of 1350 °C and pressure of 20 Pa, for 1 h. The compacts of the second powder, which was coated with SS enriched in Ni (C-WC2), were sintered at the same pressure and holding time, but at a higher temperature, 1500 °C. The compacts of the conventional mixture (M-WC) were also vacuum sintered at 1320 °C, during 3 h, at 20 Pa, and then hot isostatic pressed at 1400 °C, for 90 min, at 135 MPa, in order to reach almost full density. Three to five sintered samples per composition were prepared. The chemical characterization of sintered specimens was carried out by energy dispersive spectroscopy (EDS, detector Rontec-EDR288/SPU2) and electron microprobe analysis (EPMA-SX50, Cameca) was complementary used. The final carbon content of sintered specimens was evaluated by an automatic direct combustion (LECO CS 200 IH). The density was determined by the Archimedes' method, using ethilenoglycol.

The phase identification was performed by X-ray diffraction (XRD, Rigaku PMG-VH) and the average size of η-phase crystallites, D_C, was estimated from the Scherrer equation, $D_C = K\lambda/(\beta \cos\theta)$, where λ represents the X-ray wavelength, θ the Bragg angle, β the peak width at half-maximum corrected for instrumental broadening, and $K = 0.9$. The phase quantification results from the Rietveld analysis of XRD spectra with the aid of the GSAS suite [17]. The WC and η-phase quantification were performed with the structure parameters available in the bibliography for the hexagonal WC crystalline phase [18] and the cubic η-phase Fe_3W_3C [19] and neglecting the other minor phases.

The microstructure characterization was performed with scanning electron microscopy (SEM, Hitachi-S4100) on polished and chemically etched surfaces with Murakami's reagent (a solution of potassium ferricyanide (10 g) and sodium hydroxide (10 g) in distilled water (100 ml)). The WC average grain size was measured using the linear intercept method [20] on the micrographs and at least 300 intercepts per sample were used. The Fullman relation was applied to transform the two-dimensional mean intercept in a three-dimensional mean grain size, G [21].

The composites were mechanically characterized using depth-sensing indentation equipment (Fischerscope H100) [22–24]. In order to have representative average values for the evaluated properties, 100 tests were performed in each sample. In testing, the load is increased in steps until a nominal load of 500 mN is reached. The number of steps used for loading and unloading was 60 and the time between steps was 0.5 s. The first load step is always equal to 0.4 mN; for subsequent steps, the value of the load increment between two consecutive steps, $\Delta P_i = P_i - P_{i-1}$, is such that $\sqrt{P_i} - \sqrt{P_{i-1}}$ is constant. Two creep periods of 30 s were performed during the tests: at maximum load and at the lowest load during unloading (0.4 mN). The values of the 100 tests made in each sample were used for the direct determination of the hardness, H, and calculation of the Young's modulus, E, and of the yield stress, σ_y, using a reverse analysis approach [25]. For comparison with previously reported results, hardness measurements (HV30) were also made using a Vickers diamond indentor (293 N load). An average of 10 measurements from randomly selected areas of the sample was taken as the average hardness value of the sample. The fracture toughness, K_C, was also determined from the measurements of the Palmqvist radial cracks at the corners of Vickers hardness indentations (load, 98 N), using the formula [26]:

$$K_C = 0.087\sqrt{HW} \quad (1)$$

where $W = P/L_T$, P is the applied load and L_T the total length of cracks. The total crack length formed on the four corners of the diamond indent was measured using an optical microscope (Zeiss, Jenaphot 2000) at 400× magnification. The average of 10 indentation values was used for calculation.

3. Results and discussion

3.1. Chemical composition, atomic structure and microstructure

The chemical composition of the sintered composites, concerning Fe, Ni, Cr and C, was evaluated by EPMA and LECO and is presented in Table 1. The composites of C-WC1 powder have a binder composition similar to SS and a total binder amount of ∼6 wt.% (Table 1), assuming for the total binder amount the addition of Fe, Ni and Cr contents, the main constituents of the binder phase and neglecting other minor elements, such as Mn, Si, P, S and C (representing approximately 2 wt.% of the SS composition). The composites of C-WC2 powder possess higher binder amount (∼9 wt.%) and Ni content (∼7 times superior to C-WC1). Another composites from coated powders (C-WC3) were also considered, in spite of their microstructure and mechanical properties had been already reported elsewhere [10]. C-WC3 composites have the same binder amount than C-WC1 (∼6 wt.%), but a much higher Ni content, Table 1. The variation of the ratio between the elements with and without affinity to carbon in the binder composition of hard metal was proved to strongly limit the final phases [11]. Therefore, in the

Table 1
Final binder elements and carbon contents.

Sample	Fe[a] (wt.%)	Ni[a] (wt.%)	Cr[a] (wt.%)	Total (wt.%)	C[b] (wt.%)	Ni/(Fe + Cr)
C-WC1	4.3	0.6	1.0	5.9	5.09	0.1
C-WC2	3.9	4.4	1.0	9.3	5.27	0.9
C-WC3	1.3	4.3	0.4	6.0	5.40	2.5
M-WC	7.8	2.0	2.5	12.3	–	0.2

[a] EPMA.
[b] LECO analysis.

present study, the suitable variation of the ratio Ni/(Fe + Cr), from 0.1 to 2.5, Table 1, was used to obtain differences in the composite phase structure, namely in what concerns the percentage of η-phase. Samples of conventional powder mixture, with ∼12 wt.% of SS (Table 1) were also investigated.

The reactive sintering of the WC powders coated with SS was already systematically investigated [9,12], highlighting the higher sinterability and reactivity of the coated powders when compared with conventional mixed ones. The higher sinterability enables the achievement of near full densification in coated powders vacuum sintered, ensuring that weight losses are controlled [12]. Therefore, C-WC1 reached ∼99% of relative density at 1350 °C, 1 h, whereas an equivalent densification was also attained for C-WC2, at a higher temperature of 1500 °C. The increase of Ni in the binder composition of C-WC2 obliges to increase the sintering temperature, related to the highest eutectic temperature and to the reported lower solubility of W/C in Ni rich binders [27]. After sintering, the conventional powder mixture reached only a relative density of 90% during vacuum sintering and it was requested to be subsequently hot isostatic pressed for further densification. This was also the case of the C-WC3 compacts, due to the high Ni percentage in the binder [10].

The XRD spectra of the C-WC1, C-WC2 and M-WC sintered samples, Fig. 1, show three different phases: WC, η-phase (M_6C) and an austenite enriched in Cr and Ni. A vestigial ferrite phase is yet detectable for C-WC1 and M-WC samples, Table 2, which is not visible in the low magnification spectra of Fig. 1. Both austenite and ferrite phases are present in very small amounts in these compacts, due to the significant η-phase formation during sintering [10]. Therefore, in the quantification of the η-phase amount by the Rietveld method [17], they could be neglected. The C-WC3 composite does not present η-phase, only WC and metallic (Me) phase were detected [10].

The results of the η-phase quantification are presented in Table 2. The C-WC1 composite has the highest amount, 17 wt.%, which is significantly reduced for C-WC2, 5 wt.%, and not detectable for C-WC3 (Table 2). This decrease of η-phase, relatively to C-WC1, is related, as previously refereed, to the increase of the Ni/(Fe + Cr) ratio in the binder composition [11]. This increase displaces and enlarges the favourable region of WC + Me to carbon amounts close to the WC stoichiometric carbon [28]. Although some decarburization has occurred during sintering (as it is highlighted by the final carbon content of C-WC1 (Table 1), that is smaller than the estimated one (5.7 wt.%), assuming only the WC and binder phases), the C-WC3 sample has a high enough Ni/(Fe + Cr) ratio to place the final composition in the WC + Me region. M-WC also presents ∼12 wt.% of η-phase (Table 2). In spite of the low SS binder amount in C-WC1, the M_6C content is higher than in M-WC due to the increased reactivity of coated powders, comparatively with conventional mixed powders [9,11]. For this reason, the influence of comparable η-phase contents on the final mechanical properties could not be achieved with similar binder content in coated powders and conventional mixtures.

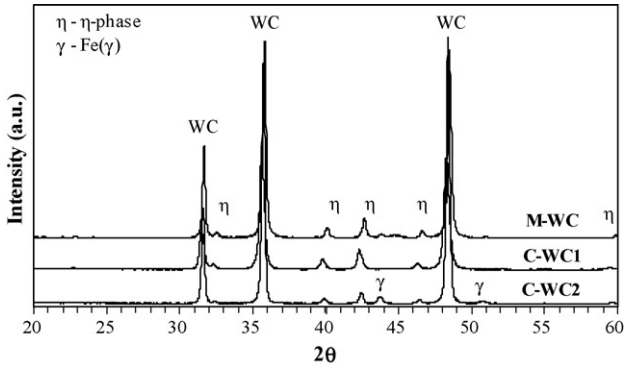

Fig. 1. XRD diffraction profiles of C-WC1, C-WC2 and M-WC samples.

Table 2
XRD data of sintered powders.

Sample	(η/(η + WC)) (wt.%)	fcc, γ	bcc, α	D_C[a] (nm)
C-WC1	17	Vestigial (+)	Vestigial	26
C-WC2	5	Small (++)	Not detected	–
C-WC3	0	∼6 wt.%	Not detected	–
M-WC	12	Vestigial (+)	Vestigial	40

[a] Average size of η-phase crystallites.

The microstructure of C-WC1 sintered sample is presented in Fig. 2(a), where, after a short etching with Murakami's, two different phases are distinguished. The major gray phase is attributed to WC and the other phase is mainly η-phase. However, a darker gray colour is observed around the contours of WC grains, which may correspond to the binder phase. The η-phase seems well adapted to the WC grains because the vestigial binder phase, that is viscous at sintering temperatures, spreads between WC and η-phase. This observation was already reported by Jia et al. [29] that also detected a binder film between WC and η grains in the three-phase region of WC–Co system. A preliminary EDS analysis was performed in the points indicated in Fig. 2(a) and is listed in Table 3. The elements detected and the atomic content confirm the presence of the $(M,W)_6C$ phase with a stoichiometry $(Fe_{2.3}Ni_{0.3})(Cr_{0.6}W_{2.8})C$. The chemical composition of this phase was also confirmed by EPMA and remains constant, within the experimental error, for different sintering temperatures and SS binder contents, as already reported [11].

The microstructure of the sample C-WC2 is presented in Fig. 2(b). Among the WC grains the two secondary phases can be distinguished: a darker phase surrounding the WC grains (binder phase) and whiter areas (η-phase). For comparison, the microstructure without η-phase (C-WC3) is also shown in Fig. 2(c), where it can be observed that the WC grain morphology is quite different from the others (C-WC1 and C-WC2): rounded for C-WC1 and C-WC2 and angular for the enriched Ni binder composite (C-WC3). Several authors [30,31] have already

Table 3
EDS analysis performed on C-WC1 sample (atomic percentages).

Point	W	Fe	Cr	Ni
A	43.0	40.1	10.6	6.3
B	44.6	39.1	11.0	5.3
C	49.2	35.7	9.7	5.4

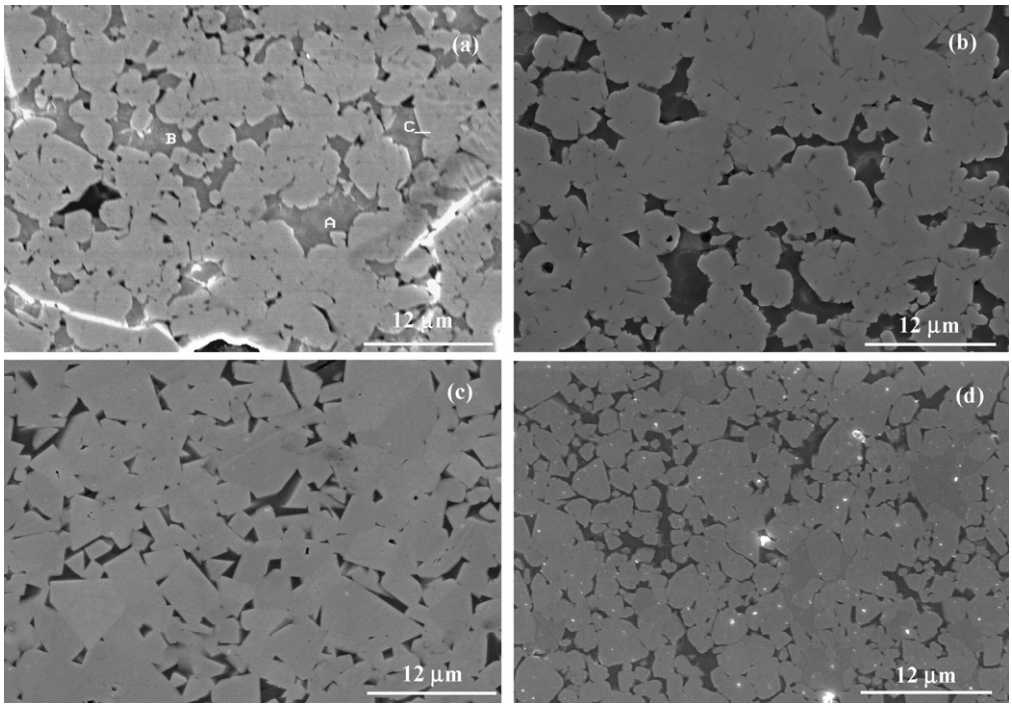

Fig. 2. SEM micrographs of (a) C-WC1, (b) C-WC2, (c) C-WC3, and (d) M-WC samples.

reported that the growth rate and the morphology of the WC interfaces change with the binder composition. Accordingly, the WC grains appear slightly rounded when the binder is enriched in W. The solubility of W in Ni and Fe at 1350 °C was reported to be 5 and 9 wt.%, respectively [27]. Therefore, rounded WC grains are expected for iron rich binders, as in C-WC1 and C-WC2. The microstructure of M-WC is similar to C-WC1 and C-WC2 (Fig. 2(d)). The average grain size, presented in Table 4, is similar for the different composites, showing a slight trend to increase for the Ni enriched compositions that were sintered at higher temperatures.

The X-ray maps of elements are shown in Fig. 3, for the C-WC1 composite. Fe and Cr are concentrated around the WC grains, in the regions correspondent to the η-phase and to the vestigial Me phase. Ni is present in lower quantity than Fe and Cr (see Table 1) and seems to be well dispersed either in the secondary phases or in the WC matrix grains (the solubilization of some Ni in the WC grains was already suggested in relation with the mechanical properties, in a previous work [10]). Moreover, the W X-ray map shows a marked reduction of intensity in the $(M,W)_6$ regions, where taking the EDS/EPMA analysis, Table 3, a significant fraction of this element must be present. This effect suggests that the η-phase must be finely divided to give a weaker signal for W, than the presumed one. The average size of η-phase crystallites, D_C, estimated from the Scherrer equation, is very small for the sample C-WC1, ∼26 nm, comparatively with the sample M-WC with ∼40 nm (Table 2), a value near of the measurable limits. The D_C value of C-WC2 cannot be properly calculated due to the small peak intensity of η-phase.

3.2. Mechanical characterization

The mechanical characteristics of the composites are presented in Table 4. The Young's modulus, E, follows the expected trend, decreasing with the increase of the binder content for all the tested samples. The yield strength, σ_y, is lower for the samples with higher Ni content, C-WC2 and C-WC3. As previously reported [10], enhanced Ni diffusion to WC in sputtered powders can be responsible for the observed decrease of the mechanical properties.

The hardness determined by depth-sensing, H (Table 4) shows decreasing values with the increase of the binder and Ni amount in the composition, Table 1. Therefore, the lowest value is observed for C-WC2 with simultaneously high Ni, 4.4 wt.%, and binder amount, 9.3 wt.%. The values of HV30, Table 4, are

Table 4
Physical and mechanical characteristics of composites prepared from coated powders and conventional mixture.

Samples	Density (g cm^{-3})	$\bar{G}$ (μm)	E (GPa)	σ_y (GPa)	H (GPa)	HV30	K_C[a] (MPa m$^{1/2}$)
C-WC1	14.0	3.0	545 ± 6	6.07	21.3 ± 0.4	1840 ± 70	9.7 ± 1.1
C-WC2	13.5	3.5	495 ± 11	4.07	15.0 ± 0.5	1400 ± 80	12.8 ± 1.2
C-WC3	14.8	4.3	520 ± 9	4.01	16.5 ± 0.4	1570 ± 90	9.8 ± 0.4
M-WC	12.8	3.0	–	–	–	1330 ± 50	12.5 ± 1.8

[a] Fracture toughness determined from measurements of the Palmqvist radial cracks.

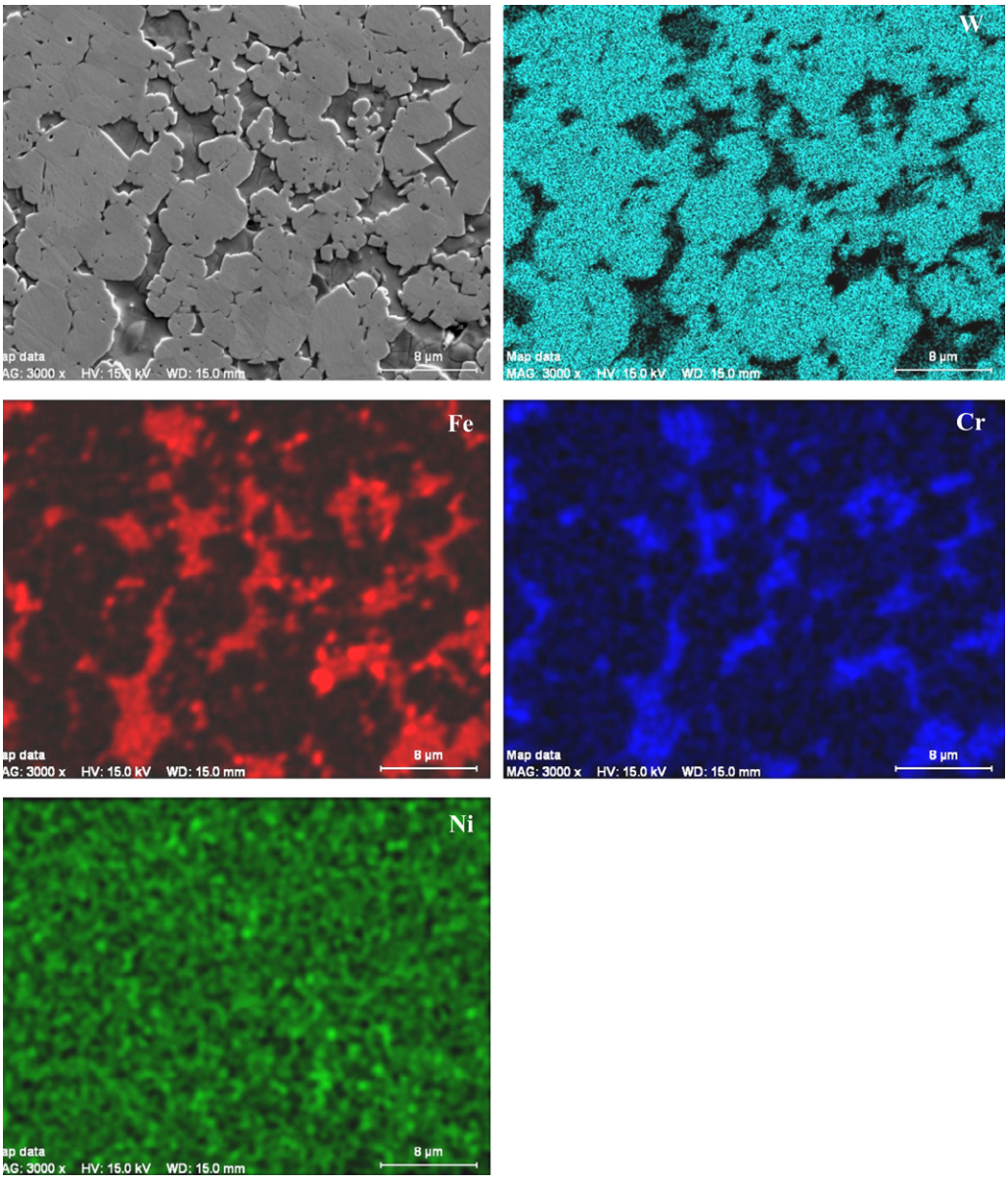

Fig. 3. SEM-SE micrograph of C-WC1 sample and respective X-ray maps of elements.

not comparable with those of H, due to the very different testing loads (see Section 2) but the same trend is observed. Toughness measurements show higher values related to increasing binder amounts (Table 4). The values for C-WC2 and M-WC are similar, within the experimental error, although the conventionally prepared sample, M-WC, possesses a larger binder percentage, without presenting significant difference on the average WC grain size, Table 4.

In Fig. 4(a) and (b) the representation of fracture toughness, K_C, vs. HV30 was chosen to further analyse the effect of the composition and processing conditions on the mechanical behaviour of the tungsten carbide composites here developed and to compare the measured values with results for WC–Co and WC–SS composites, reported in the bibliography [32,33] and compiled in Table 5. In Fig. 4(a) three groups of cemented carbide, within medium/coarse range, were distinguished: WC–Co composites (from 6 to 15 wt.% Co) with the lowest values of K_C for the same hardness [32]; WC–SS composites from the bibliography [33] together with M-WC, all conventionally prepared, with intermediate values of K_C for equivalent hardness; finally, the results for composites from coated powders, presenting the highest relation between K_C and HV30, were grouped, despite the differences in their binder compositions. The decrease of K_C with hardness was foreseeable for the three groups of composites: the harder a material more brittle it is. However, the relation between hardness and toughness is higher for the composites with SS binder when compared with the ones with Co, all using conventionally prepared powders. Therefore, in terms of the considered properties, the already reported advantages of SS for Co substitution [33,34], is here reinforced. It may also be noted that the point correspondent to M-WC support very well those from literature, despite the fact that this composite possesses a very significant amount of η-phase, ∼12 wt.%, whereas those from

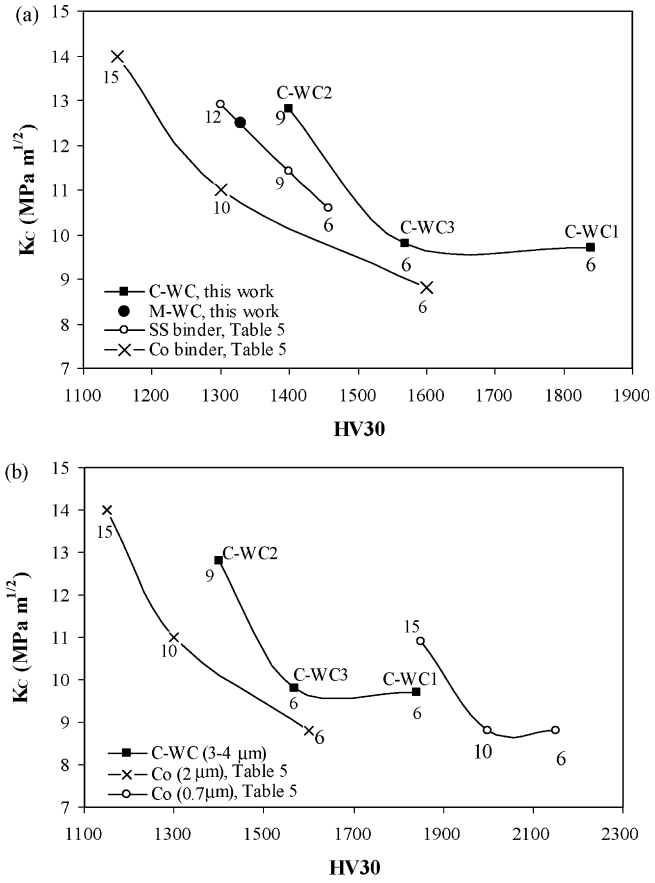

Fig. 4. Variation of K_C with Vickers hardness for hardmetals with different binder compositions (the numbers indicate the binder amount (wt.%)): (a) effect of composition and processing method for medium/coarse grain sizes ($\bar{G} > 2$ mm); (b) effect of composition and grain size.

literature are reported to be free of η-phase [33]. Moreover, the composites from coated powders show yet higher values of K_C for the same hardness, when compared with the conventionally prepared composites, in Fig. 4(a). A higher uniformity of the binder distribution was already shown to persist, even after sintering, in the composites from coated powders [10]. Additionally, the smaller crystallite size of the second phases formed from the sputtered binder during sintering, Table 2, contributes also for the higher toughness. The grain size should be reduced to a range of submicron size to attain K_C and HV30 values similar to C-WC1 in WC/Co cemented carbides, as shown in Fig. 4(b).

Regarding the effect of the η-phase on the reported mechanical properties of the coated powders, the reduction of the M_6C phase from ~17 wt.% in C-WC1 to non-detectable values (<2 wt.%) in C-WC3, with the total binder content constant, had a clear reduction of hardness without any benefit of toughness, Fig. 4(a) and Table 2. Some authors [34,35] have already stated that η-phase enhances hardness and abrasion resistance in WC composites with ultrafine grains. In fact, the binder phase of C-WC1 sample is vestigial, so the most representative region is WC + M_6C phases, which could explain the high hardness. Furthermore, a high toughness (K_C) was attained in the C-WC2 composite, although it was estimated to have ~5 wt.% of η-phase. However, the toughness was expected to degrade with the substitution of the ductile binder phase by the brittle η-phase [14,15], but this effect was not here observed. Phase composition and microstructure suggested that the studied composites have different contributions, resulting from the presence of the previous coating on powders, such as: (i) spreading of the ductile binder phase into the WC and M_6C junctions, Fig. 2, due to its good wettability at the sintering temperatures, and favoured by the high uniform distribution in the coated powders; (ii) the nanocrystalline size of η-phase, Table 2, and the fine dispersion of the η-phase, Fig. 3. These aspects need, however, further investigation to be confirmed, namely using TEM analysis in forthcoming studies.

Therefore, the WC coated powders with iron rich binders are interesting to prepare cemented carbide that requires high hardness, using small amounts of coating binder. Besides, the relative high cost of the coated powders production can be balanced with the manufacturing cost reduction, coming from the elimination of the milling and dewaxed steps and the decreasing of sintering temperatures, without the need of HIP to obtain complete dense compacts. The use of coarse grain sizes is also an economical benefit, since equivalent properties to the ultrafines ones were obtained, reducing the milling time and energy.

Table 5
Literature results for WC composites using stainless steel (SS) and cobalt (Co) binders.

Binder (wt.%)	$\bar{G}$ (μm)	HV30	K_C (MPa m$^{1/2}$)	Ref.
6 Co	2.2	1600	8.8	[32]
10 Co	2.2	1300	11	[32]
15 Co	2.2	1150	14	[32]
6 Co	0.7	2150	8.8	[32]
10 Co	0.7	2000	8.8	[32]
15 Co	0.7	1850	10.9	[32]
6 SS	4.1	1458	10.6	[33]
9 SS	4.5	1398	11.4	[33]
12 SS	5.1	1300	12.9	[33]

4. Conclusions

The composites of WC powders coated by sputtering with SS or Ni enriched SS binders show a good compromise between toughness and hardness, better than composites of similar composition and grain size, conventionally prepared.

The η-phase formed in these composites increases the hardness without loss of toughness, which was attributed to specific microstructural and structural characteristics, as the spreading of the ductile binder phase in the WC/η-phase junctions and the nanocrystalline structure and fine dispersion of the formed η-phase.

SS binders are promising substitutes for Co, taking into account the relation between toughness and hardness. Superior values for these properties were found mainly in composites prepared from coating powders with nanocristalline iron enriched coatings, making these composites attractive for

applications where high hardness and moderate toughness are the targets.

Acknowledgements

The authors wish to thank Bsc A.M. Jesus for the help in the toughness measurements. The author C.M.F. gratefully acknowledges the financial support of the POCTI programme of the Portuguese Foundation for Science and Technology (FCT) and European Social Fund (FSE).

References

[1] R.K. Viswanadham, P.G. Lindquist, Transformation-toughening in cemented carbides. Part I. Binder composition control, Metall. Trans. A 18A (1987) 2163–2173.
[2] T. Kakeshita, C.M. Wayman, Martensitic transformations in cements with a metastable austenitic binder, Mater. Sci. Eng. A141 (1991) 209–219.
[3] B. Uhrenius, Phase diagrams as a tool for production and development of cemented carbides and steels, Powder Metall. 35 (3) (1992) 203–210.
[4] R. González, J. Echeberría, J.M. Sánchez, F. Castro, WC–(Fe, Ni, C) hardmetals with improved toughness through isothermal heat treatments, J. Mater. Sci. 30 (13) (1995) 3435–3439.
[5] R. Cooper, S.A. Manktelow, F. Wong, L.E. Collins, The sintering characteristics and properties of hard metal with Ni–Cr binders, Mater. Sci. Eng. A A105–A106 (1988) 269–273.
[6] V.A. Tracey, Nickel in hardmetals, Int. J. Refract. Met. Hard Mater. 11 (1992) 137–149.
[7] C.M. Fernandes, V.M. Ferreira, A.M.R. Senos, M.T. Vieira, Stainless steel coatings sputter-deposited on tungsten carbide powder particles, Surf. Coat. Technol. 176 (1) (2003) 103–108.
[8] C.M. Fernandes, A.M.R. Senos, M.T. Vieira, Particle surface properties of stainless steel-coated tungsten carbide powders, Powder Technol. 164 (2006) 124–129.
[9] C.M. Fernandes, A.M.R. Senos, M.T. Vieira, Sintering of tungsten carbide particles sputter-deposited with stainless steel, Int. J. Refract. Met. Hard Mater. 21 (2003) 147–154.
[10] C.M. Fernandes, A.M.R. Senos, M.T. Vieira, J.M. Antunes, Mechanical characterization of composites prepared from WC powders coated with Ni rich binders, Int. J. Refract. Met. Hard Mater. 26 (2008) 491–498.
[11] C.M. Fernandes, A.M.R. Senos, M.T. Vieira, Control of eta carbide formation in tungsten carbide powders sputter-coated with (Fe/Ni/Cr), Int. J. Refract. Met. Hard Mater. 25 (2007) 310–317.
[12] C.M. Fernandes, A.M.R. Senos, M.T. Vieira, Study of sintering variables of tungsten carbide particles sputter-deposited with stainless steel, Mater. Sci. Forum 455–456 (2004) 295–298.
[13] A.P. Miodownik, Means of predicting structure and performance of new materials, Powder Metall. 32 (4) (1989) 269–276.
[14] D. Moskowitz, M.J. Ford, M. Humenik, High-strength tungsten carbides, Mod. Dev. Powder Metall. 5 (1970) 225–234.
[15] D. Moskowitz, M.J. Ford, M. Humenik, High-strength tungsten carbides, Int. J. Powder Metall. 6 (4) (1970) 55–64.
[16] H.J. Goldschmidt, The structure of carbides in alloy steels. Part II—carbide formation in high-speed steels, J. Iron Steel Inst. 170 (1952) 189–204.
[17] A.C. Larson, R.B. Von Dreele, LAUR 86-748 Report, General Structure Analysis System, Los Alamos National Laboratory, 1990.
[18] J. Leiciejewicz, A note on the structure of tungsten carbide, Acta Cryst. 14 (1961) 200.
[19] Q. Yang, S. Andersson, Application of coincidence site lattices for crystal structure description. Part I. $\Sigma = 3$, Acta Cryst. B43 (1987) 1–14.
[20] J.M. Antunes, L.F. Menezes, J.V. Fernandes, Ultra-microhardness testing procedure with Vickers indenter, Surf. Coat. Technol. 149 (1) (2002) 27–35.
[21] B. Roebuck, E.G. Bennett, M.G. Gee, Grain size measurement methods for WC/Co hardmetals, in: H. Bildstein, R. Eck (Eds.), Proceedings of the 13th International Plansee Seminar, vol. 2, Metallwerk Plansee, Reutte, 1993, p. 273.
[22] D. Newey, M.A. Wilkins, H.M. Pollock, An ultra-low-load penetration hardness tester, J. Phys. E: Sci. Instrum. 15 (1982) 119–122.
[23] J.L. Loubet, J.M. Georges, G. Meille, Vickers indentation curves of elastoplastic materials, in: P.J. Blau, B.R. Lawn (Eds.), Microindentation Techniques in Materials Science and Engineering, ASTM STP, 889, American Society for Testing and Materials, Philadelphia, PA, 1986p. 72.
[24] W.C. Oliver, G.M. Pharr, An improved technique for determining hardness and elastic modulus using load and displacement sensing indentation, J. Mater. Res. 7 (6) (1992) 1564–1583.
[25] J.M. Antunes, J.V. Fernandes, L.F. Menezes, B.M. Chaparro, A new approach for reverse analyses in depth-sensing indentation using numerical simulation, Acta Mater. 55 (1) (2007) 69–81.
[26] C.B. Ponton, R.D. Rawlings, Vickers indentation fracture toughness test. Part 1. Review of literature and formulation of standardised indentation toughness equations, Mater. Sci. Technol. 58 (1989) 865–872.
[27] B. Uhrenius, K. Forsen, B.O. Haglund, I. Andersson, Phase-equilibria and phase-diagrams in carbide systems, J. Phase Equilib. 16 (5) (1995) 430–440.
[28] A.F. Guillermet, An assessment of the Fe–Ni–W–C phase diagram, Metallkund 78 (3) (1987) 165–171.
[29] K. Jia, T.E. Fisher, B. Gallois, Microstructure, hardness and toughness of nanostructured and conventional WC–Co composites, Nanostruct. Mater. 10 (5) (1998) 875–891.
[30] V. Chabretou, C.H. Allibert, J.M. Missiaen, Quantitative analysis of the effect of the binder phase composition on grain growth in WC–Co sintered materials, J. Mater. Sci. 38 (2003) 2581–2590.
[31] Y. Wang, M. Heusch, S. Lay, C.H. Allibert, Microstructure evolution in the cemented carbides WC–Co. I. Effect of the C/W ratio on the morphology and defects of the WC grains, Phys. Status Solidi (a) 193 (2) (2002) 271–283.
[32] J.L. Chermant, F. Osterstock, Fracture toughness and fracture of WC–Co composites, J. Mater. Sci. 11 (1976) 1939–1951.
[33] T. Farooq, T.J. Davies, Tungsten carbide hard metals cemented with ferroalloys, Int. J. Powder Metall. 27 (4) (1991) 347–355.
[34] G.S. Upadhyaya, S.K. Bhaumik, Sintering of submicron WC–10%Co hard metals containing nickel and iron, Mater. Sci. Eng. A105–A106 (1988) 249–256.
[35] M. Bergström, The eta-carbides in the quaternary system Fe–W–C–Cr at 1250 °C, Mater. Sci. Eng. 27 (1977) 271–286.